

Numerical simulations of the linear drift memristor model

Fabiano A.S. Ferrari^{1,2,a}, Thiago L. Prado¹, Thiago F.P. da Silva¹, Clara M. dos Santos¹, Moises S. Santos³, Silvio L.T. de Souza⁴, Kelly C. Iarosz⁵, José D. Szezech Jr.^{2,6}, and Antonio M. Batista^{2,6}

¹ Institute of Engineering, Science and Technology, Federal University of Jequitinhonha and Mucuri's Valleys, Janaúba, Brazil

² Graduate Program in Science, State University of Ponta Grossa, Ponta Grossa, Brazil

³ Department of Physics, Federal University of Paraná, Curitiba, Brazil

⁴ Campus Centro-Oeste, Federal University of São João del-Rei, Divinópolis, Brazil

⁵ Institute of Physics, University of São Paulo, São Paulo, Brazil

⁶ Department of Mathematics and Statistics, State University of Ponta Grossa, Ponta Grossa, Brazil

Received: 4 October 2018 / Revised: 4 December 2018

Published online: 15 March 2019

© Società Italiana di Fisica / Springer-Verlag GmbH Germany, part of Springer Nature, 2019

Abstract. Memristor is a passive element theoretically proposed by Leon Chua in the 1970's. It started to receive attention after 2008, when researchers from the HP Labs presented a device with memristive properties. Since then, several models have been proposed to describe the memristor. In this work, we analyze the linear drift model, comparing the numerical solutions with analytical solutions and SPICE simulations. We demonstrate that different solutions can be found depending on the method and parameter set.

1 Introduction

In 2008, Strukov *et al.* (HP Labs) published a paper entitled “The missing memristor is found” in *Nature* [1], where they claimed to have built a device with memristive properties. Memristor was theoretically proposed by Leon Chua in 1971 [2], it is an element that behaves like a resistor but the resistance varies according to the history of voltages applied on it. The name memristor means resistor with memory, in this case, the dependence on the past states is considered as a memory property. The main application of memristor is in computation. In combination with transistors, they are expected to improve performance of digital circuits without shrinking transistors [3]. Recently, a memristor-based hardware to perform a high precision computing task was proposed [4]. Memristors can be used as ultra dense non-volatile memory [5, 6], artificial synapse [6, 7], detection of weak signals [8], suppression of chaotic ferroresonance [9] and optimization of microwave passive circuits [10].

In electronics, the elements can be divided into passive and active elements. Active elements can increase the power of a signal, on the other hand, passive elements cannot, usually, causing loss of power [11]. There are four basic passive elements: resistor, capacitor, inductor and memristor (recently introduced). All other passive elements can be built from the four basic elements. Here, we are accepting memristor as a basic passive element, however, it is not a consensus in the literature and it is still a subject of debate [12–14]. The passive elements are characterized by four elementary physical quantities: charge q , voltage V , electrical current i and magnetic flux ϕ . The relation between the passive elements and elementary physical quantities are presented in fig. 1(a).

The most fundamental element is the resistor, as shown in fig. 1(b), it is a two-terminal element able to transform the electric current in heat, causing a resistance in the current flow [15]. The amount of resistance R can be quantified through the Ohm's Law: $dV = R di$. The capacitor, represented in fig. 1(c), is a two-terminal element able to store energy in the electric field, it is characterized by the capacitance C . The capacitance can be obtained from the relation: $dq = C dV$. The inductor is a two-terminal element able to store energy in the magnetic field. Different from resistors and capacitors, inductors require alternate current to operate, as represented in fig 1(d). They are characterized by the inductance L , obtained from the relation $d\phi = L di$ [15]. Furthermore, there is a relation between charge and current, that is the basic definition of electric current, $dq = i dt$, and a relation between magnetic flux ϕ and voltage V , that is the basic definition of magnetic flux, $d\phi = V dt$. In the 1970's, Leon Chua proposed an hypothetical element

^a e-mail: fabianosferrari@gmail.com

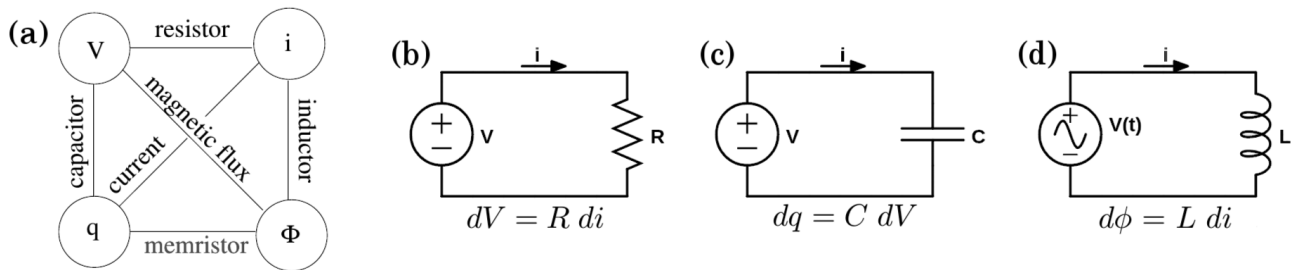


Fig. 1. (a) Relation between the fundamental variables and basic passive elements, (b) power source + resistor circuit, (c) power source + capacitor circuit, and (d) power source + inductor circuit.

associated with the relation between charge q and magnetic flux ϕ . This element (latter called memristor) would be characterized by a constitutive relation $d\phi = M dq$. We can re-write the constitutive relation in terms of the other quantities, in this case:

$$V dt = M i dt, \quad (1)$$

this means that, M and R have the same unit. Due to its dependency on the past states of current and voltage, the element that satisfies eq. (1) works as a resistor with memory.

The first model to explain the memristor behavior is the linear drift model [1]. This qualitative model assumes that free particles move in the memristor according to a linear drift movement. Experimental results, however, demonstrate that, the free particles should move in a non-linear manner. This effect can be included in the linear drift model adding a term in the differential equation, called window function [16,17]. In memristors, the conductance alternates between two states, often called ON and OFF states. To characterize this behavior, researchers at HP Labs developed a memristor model compatible with the experimental results [18]. They showed that, in nonlinear memristors, the energy required to switch a metal-oxide device decreases exponentially with increasing applied current [18].

Currently, several models describe properties and behavior of memristor with good agreement with experimental results [19–23]. Yakopcic *et al.* presented a model that could be used to model memristor-based neuromorphic systems [19]. The circuit emulator, TEAM (ThrEshold Adaptive Memristor Model) is simple and computational efficient being adapted to Verilog-A and SPICE simulations [22]. One of the main challenges in the study of memristor properties is to define an appropriated model. In this paper, we focus on the simulation issues of the linear drift model. However, even more realistic models can present numerical errors or problems of convergence due numerical methods, and most of them require special treatments to be solved [24].

The fundamental properties that must be satisfied by a memristor model are discussed in sect. 2. In sect. 3, we present the details about the linear drift model. Despite the large number of memristor models, in this paper, we focus on the linear drift model because of the large amount of features that can be observed when different numerical methods are considered. This results are discussed in sect. 4. In sect. 5, we present our conclusions.

2 Properties of a memristor

The memristor can have a current or voltage input, when the input is the voltage, the system is voltage controlled, in a generalized form it can be described as

$$i = W(x_1, x_2, \dots, x_N)V, \quad (2)$$

$$\frac{dx_k}{dt} = f_k(x_1, x_2, \dots, x_N, V), \quad (3)$$

where $W()$ is called memductance ($W = 1/M$), $k = 1, 2, \dots, N$, where N is the number of state variables. When the input is the current, the system is current controlled, it can be described as

$$V = M(x_1, x_2, \dots, x_N)i, \quad (4)$$

$$\frac{dx_k}{dt} = g_k(x_1, x_2, \dots, x_N, i). \quad (5)$$

The memristors that satisfy $M(f_k(x_1, x_2, \dots, x_N)) = d(f_k(x_1, x_2, \dots, x_N))/dq$ are called ideal memristors [25].

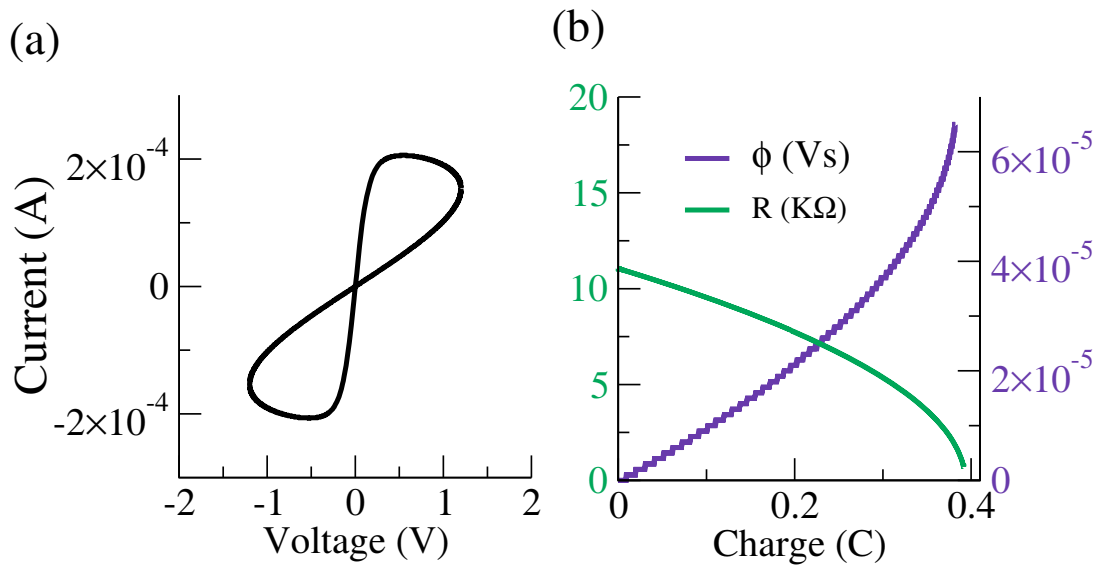


Fig. 2. Characteristics of a memristor. (a) Memristor’s pinched hysteresis loop, (b) memristor’s constitutive relations.

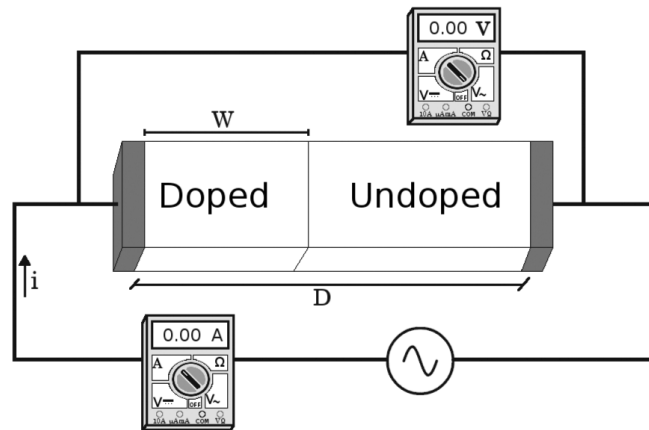


Fig. 3. Representation of TiO₂ memristor. The width of the bilayer is D meters and the doped region is w meters.

According to Leon Chua, any 2-terminal non-volatile memory device based on resistance switching can be considered as a memristor [26]. However, in order to be considered a memristor the device needs to satisfy three properties [7]:

- The voltage-current plane must describe a pinched hysteresis loop.
- The area inside the loop have to decrease as frequency ω is increased.
- In the limit $\omega \rightarrow \infty$, the voltage-current plane shall describe a straight line, indicating ohmic behavior.

Memristive behaviors are generally identified by the pinched hysteresis loop, as shown in fig. 2(a), however, the hysteresis loop varies as the frequency or the amplitude of the signal is varied. The appropriated quantities to define a memristor is the constitutive relation, $\phi = f(q)$, as shown by the purple line in fig. 2(b). The relation between memristance M and charge q can also identify a memristive signature (green line in fig. 2(b)) [26].

3 Linear drift model

The device, presented in 2008 by Strukov *et al.* [1], is composed of two layers, one doped by oxygen vacancies TiO_{2-x}, and other composed of undoped molecules of TiO₂, as represented in fig. 3. The bilayer is D meters width and the doped region is $w(t)$ meters width. When voltage is applied between the layers, the free charged particles, called dopants, move due to the electrical field, causing the variation in the size of the doped layer. This mechanism is also responsible for the memristive behaviors.

The behavior of HP TiO₂ device can be described by the system:

$$R(x) = R_{\text{ON}}x + R_{\text{OFF}}(1 - x), \quad (6)$$

$$\frac{dx}{dt} = ki(t)f(x), \quad (7)$$

where R_{ON} is the resistance of the doped region, R_{OFF} is the resistance of the undoped region, usually, $R_{\text{OFF}} \gg R_{\text{ON}}$. k is a constant that depends on the properties of the material, $i(t)$ is the applied current, $f(x)$ is called “window function” and it is an artificial argument that guarantees the solution remains in the interval of physical meaning. The variable x is the state variable, it is a normalization of the w width, such as: $x = w/D$ and $0 < x < 1$. Despite of being a qualitative description, this model is of great interest because it can be derived from physical assumptions.

In eq. (7), when $f(x) = 1$, the state variable x is proportional to the electric current $i(t)$, in this case, the dopants are assumed to move in a linear drift at speed v_D ,

$$\begin{aligned} \frac{dx}{dt} &= \frac{d(w/D)}{dt} = \frac{v_D}{D}, \\ \frac{dx}{dt} &= k \frac{dq}{dt}, \end{aligned} \quad (8)$$

where $v_D = [(\mu R_{\text{ON}})/D]i(t)$ and μ is the dopant mobility. The parameters can be grouped in a single parameter $k = \mu R_{\text{ON}}/D^2$.

The general solution of eq. (8) is

$$x(t) = x_0 + kq(t), \quad (9)$$

where x_0 is a parameter and depends on the boundary conditions. Replacing eq. (9) in eq. (6), we have

$$\begin{aligned} R(q) &= R_0 + kq(R_{\text{ON}} - R_{\text{OFF}}), \\ R(q) &= R_0 - \Delta kq, \end{aligned} \quad (10)$$

where $R_0 = R_{\text{OFF}} - x_0\Delta R$ and $\Delta R = R_{\text{OFF}} - R_{\text{ON}}$. Applying the Kirchoff's Law in the circuit of fig. 3, we have

$$v(t) = R(q) \frac{dq}{dt}, \quad (11)$$

$$\phi(t) = \int_{-\infty}^t V(\tau) d\tau, \quad (12)$$

consequently,

$$\phi(t) = R_0q - \frac{\alpha q^2}{2} + q_0, \quad (13)$$

where $\alpha = k\Delta R$. The boundary condition $q(0) = 0$, implies $q_0 = 0$. Equation (13) can be rewritten as

$$q = \frac{R_0}{\alpha} \left(1 - \sqrt{1 - \frac{2\alpha\phi}{R_0^2}} \right). \quad (14)$$

The linear drift case is defined by eqs. (13) and (14), they describe the memristor behavior when the state variable x is distant of the borders in $x = 0$ or $x = 1$. When the state variable x spends time in the vicinity of the borders, the use of a window function, $f(x) \neq 1$, is required. In this work, we used the Joglekar's window function $f_p(x)$ [17],

$$f_p(x) = 1 - (2x - 1)^{2p}, \quad (15)$$

where p is an integer parameter, $p = 1, 2, \dots, \infty$. This window function has the advantage of being simple, it can provide analytical solutions and good convergence for numerical simulations.

For the case $p = 1$, the Joglekar's window function can be rewritten as

$$f_1(x) = 1 - (2x - 1)^2 = 4x(1 - x). \quad (16)$$

Substituting eq. (16) in eq. (7), we have

$$\frac{dx}{dt} = 4kx(1 - x) \frac{dq}{dt}, \quad (17)$$

$$\frac{1}{x(1 - x)} \frac{dx}{dt} = \frac{d(4kq)}{dt}, \quad (18)$$

$$\frac{d}{dt} \ln \left\{ \frac{x}{1 - x} \right\} = \frac{d}{dt} \{4kq(t)\}, \quad (19)$$

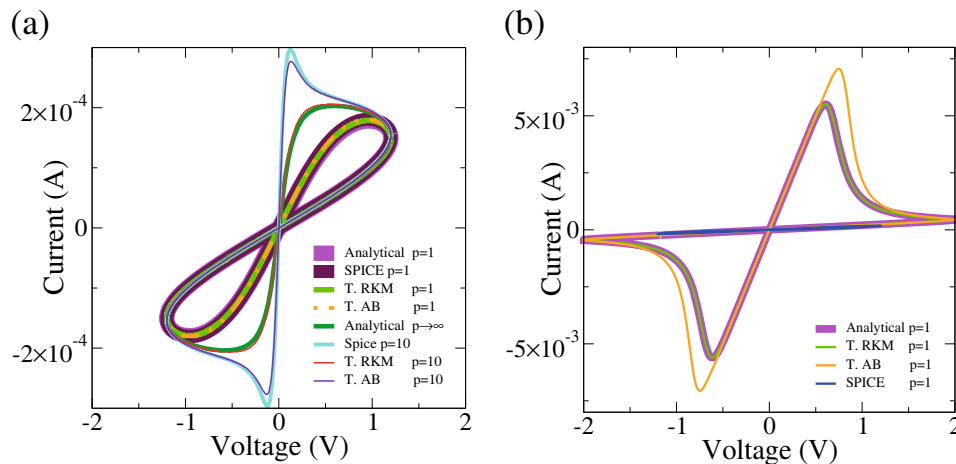


Fig. 4. Memristors’s pinched hysteresis loop: (a) linear drift case, (b) non-linear drift case. The analytical solution $p = 1$ is the solution described by eq. (21) and the analytical solution $p \rightarrow \infty$ is described by eq. (9). “T. RKM” is the Runge-Kutta-Merson solution and “T. AB” is the Adams-Bashforth solution.

consequently

$$\ln \left\{ \frac{Ax}{1-x} \right\} = \{4kq(t) + B\}, \tag{20}$$

$$x = \frac{Ce^{4kq}}{A + Ce^{4kq}}, \tag{21}$$

where $C = e^B$. The coefficients A and C must to be defined such $0 < x < 1$, in this case

$$A = 1 - x_0, \tag{22}$$

$$C = x_0. \tag{23}$$

When $p \rightarrow \infty$, the system recovers the linear drift solutions (eqs. (13) and (14)).

4 Numerical simulations

In sect. 3, we presented a qualitative model to describe the memristor behavior. In this section, we compare the analytical solutions¹ with numerical and SPICE simulations. We tested two types of numerical methods: the Runge-Kutta-Merson method, that is one-step, and the Adams-Bashforth method, that is multi-step. The details about the numerical methods and SPICE simulations are described in appendix A and B, respectively. In all simulations was used $h = 0.001$ as the integration step size. We fixed this value because it provides good results for a wide range of system parameters.

4.1 Linear drift case

The linear drift cases are those where the state variable x is distant of the borders at $x = 0$ and $x = 1$. To analyze this case, we use the same set of parameters used by Biolek *et al.* [16].

R_{ON} (Ω)	R_{OFF} (Ω)	x_0	V_0 (V)	f (Hz)
100	16000	0.25	1.2	1.0

Considering that a sinusoidal voltage, $v(t) = V_0 \sin(2\pi ft)$ is applied on the memristor, the pinched hysteresis loop for this case is shown in fig. 4(a). When the window function parameter $p = 1$, all methods present the same solution. When $p = 10$, we observe two different solutions, the SPICE and Adams-Bashforth results evolve to one solution and the analytical and the Runge-Kutta results evolve to another.

¹ The analytical solutions were first developed by Joglekar *et al.* [17].

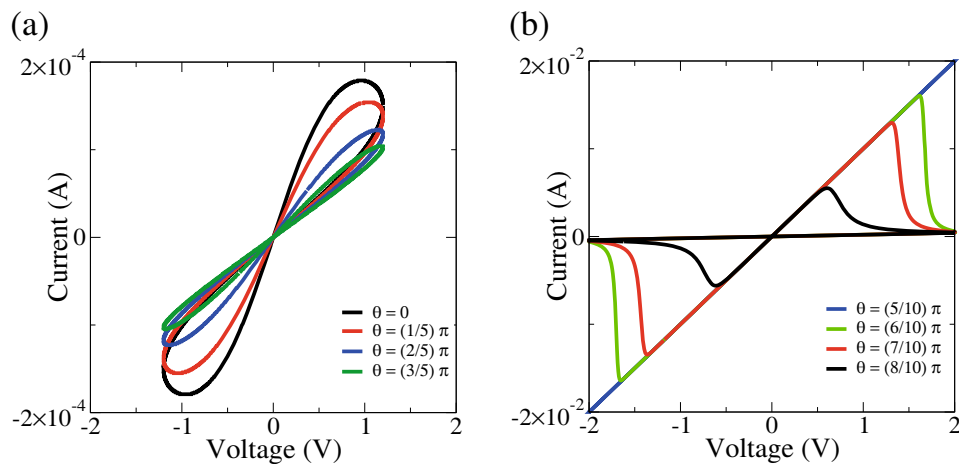


Fig. 5. Changes in the pinched hysteresis loop induced by phase: (a) linear drift case, (b) non-linear drift case. Simulations with the Runge-Kutta-Merson method.

4.2 Non-linear drift case

Aiming to reproduce the non-linear drift case, we applied a sinusoidal voltage using the appropriate set of parameters proposed by Biolek *et al.* [16]

R_{ON} (Ω)	R_{OFF} (Ω)	x_0	V_0 (V)	f (Hz)
100	5000	0.8	2.0	1.0

Different from the linear drift case, when we use $p = 10$, we do not observe the hysteresis loop, except for a very unusual set of parameters. For $p = 1$, the solutions from Runge-Kutta-Merson method matches with the analytical solution. Only setting the appropriate p parameters is not enough to observe the hysteresis loop in a robust way. The desired solution is obtained through the adjust of the applied voltage phase, *i.e.*, $v(t) = V_0 \sin(2\pi ft + \theta)$. In fig. 4(b) we see a slight difference between the solutions from the Runge-Kutta-Merson and Adams-Bashforth methods. In this case, the solution from SPICE is different from the others. Besides, depending on the parameter set other types of solutions can be observed. Sometimes, the solutions diverges, other times a straight line is observed (ohmic behavior) or, in very few cases, other types of pinched hysteresis loops appear.

4.3 The effect of phase

As occurred in fig. 4(b), variation in the voltage phase can change the area of the hysteresis loop, as shown in fig. 5(a). The phase changing can also lead to distinct solutions, as shown for the non-linear drift case in fig. 5(b). When the phase is changed to $\theta = (5/10)\pi$, the blue line in fig. 5(b), the hysteresis loop evolves to a straight line, indicating the phase can switch the system from a memory to a memoryless state.

4.4 Unexpected solutions using Adams-Bashforth method

Some unexpected results appear when the amplitude of the voltage is varied. As shown in fig. 6(a), as the voltage is varied the hysteresis loop rotates and goes to the second and fourth quadrant. This effect is not verified when Runge-Kutta-Merson method is used. A similar behavior happens when the sinusoidal voltage is replaced by a triangular wave voltage, as shown in fig. 6(b). In these cases, the area of the hysteresis loops varies in a nonuniform manner. The hysteresis loop in the second and fourth quadrants indicates the memristor is behaving as an active element [26]. As memristors are passive elements, these type of solutions have no physical meaning.

4.5 Distortions due time evolution using Runge-Kutta-Merson method

Differences between Adams-Bashforth and Runge-Kutta-Merson methods are observed when we analyze the time evolution of the solution. For the Runge-Kutta-Merson and the analytical solution, the hysteresis loop change as time evolves. Black lines in figs. 7(a) and (b) describe the distortions for the linear and non-linear drift cases. In both cases the pinched hysteresis loop evolves to a straight line. The deformation of the hysteresis loop is slow for the linear case and fast for the non-linear case. The solutions from Adams-Bashforth method, on the other hand, remains in stationary state after a short transient time.

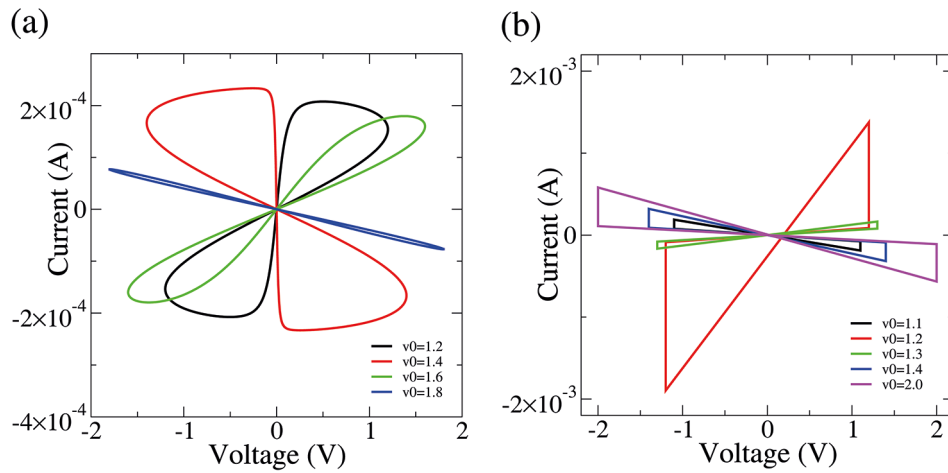


Fig. 6. Effect of varying the amplitude in the linear drift case (a) of the sinusoidal voltage and (b) of the triangular wave voltage.

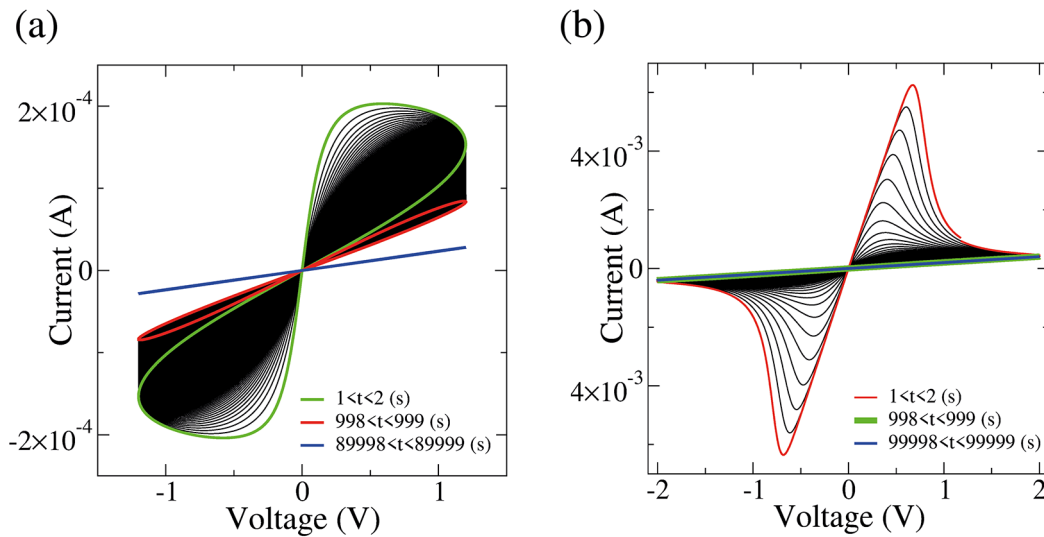


Fig. 7. Distortions due to time evolution: (a) linear drift case, (b) non-linear drift case.

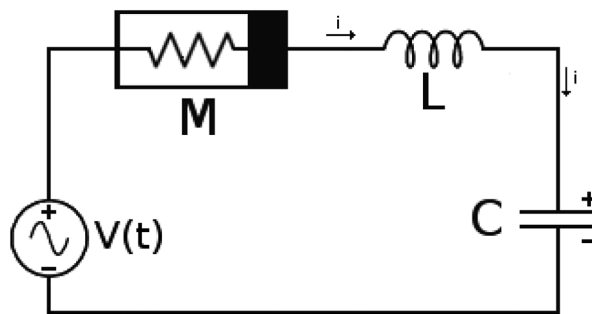


Fig. 8. MLC circuit representation.

4.6 MLC circuit

From this point is clear that Adams-Bashforth and Runge-Kutta-Merson can provide different solutions, however, what happens when we analyze the memristor behavior in a circuit? To answer this question we compare the methods in a MLC circuit. In this case, the memristor is coupled in series with an inductor and a capacitor, as shown in fig. 8.

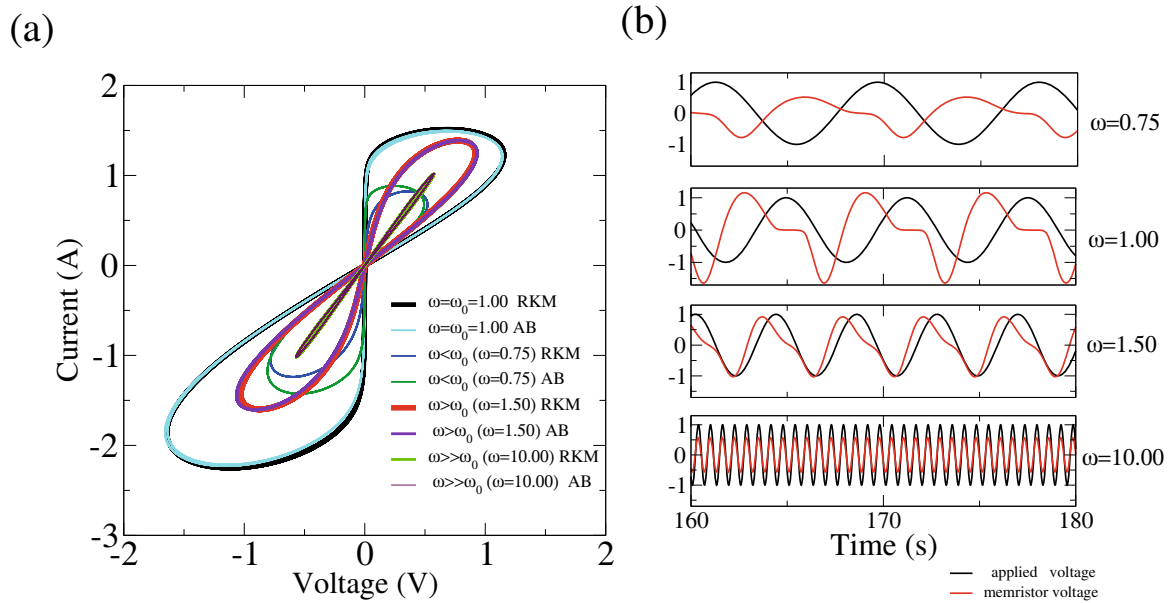


Fig. 9. (a) Pinched hysteresis loop for a memristor in a MLC circuit, (b) comparison between applied and memristor voltage in the MLC circuit. RKM —Runge-Kutta-Merson method, AB —Adams-Bashforth method.

Applying the Kirchoff laws, the differential equation that describes the system is given by

$$L \frac{di(t)}{dt} + Mi(t) + v(0) + \frac{1}{C} \int_0^t i(\tau) d\tau = v(t), \quad (24)$$

where L is the inductance, C is the capacitance, M is the memristance and $v(t)$ is the applied voltage. To solve eq. (24) we differentiate it with respect to t

$$L \frac{d^2i(t)}{dt^2} + M(t) \frac{di(t)}{dt} + \frac{i(t)}{C} = \frac{dv(t)}{dt}. \quad (25)$$

We separate the second-order differential equation of eq. (25) into two first-order differential equations,

$$z(t) = \frac{di(t)}{dt}, \quad (26)$$

$$\frac{dz(t)}{dt} = \frac{1}{L} \left(-M(t)z(t) + \frac{dv(t)}{dt} \right) - \frac{i(t)}{\omega_0^2}, \quad (27)$$

where $\omega_0 = 1/\sqrt{LC}$ is the resonant frequency of the RLC circuit [27].

In our analysis, we apply a sinusoidal voltage in the circuit, $v(t) = v_0 \sin(\omega t)$, and the memristance $M(t)$ is described by eqs. (6) and (7). We observe that, there are no solutions for $R_{ON} \sim R_{OFF}$, and when R_{ON} is reduced the system exhibits pinched hysteresis loop, as shown in fig. 9(a). For $R_{ON} \ll R_{OFF}$ the memristor behaves as a simple resistor, hence the circuit behaves like a RLC circuit. To simulate the circuit of fig. 9 we used the following parameter set

R_{ON} (Ω)	R_{OFF} (Ω)	x_0	v_0 (V)	p	L (H)	C (F)
0.002	2	0.5	1.0	10	1	1

When the Adams-Bashforth method is used, besides the window function, it is necessary to include the conditions:

$$\begin{aligned} \text{if } x > 0.99, & \quad \text{then } x = 0.99, \\ \text{if } x < 0.01, & \quad \text{then } x = 0.01, \end{aligned} \quad (28)$$

otherwise the solution will diverge, the solutions are exhibited in fig. 9(a). A mismatch between the methods appear when $\omega < \omega_0$. As expected for memristor, its behavior evolves to a resistor when the frequency of the applied voltage is increased. The area of the hysteresis loop reaches a maximum at $\omega = \omega_0$, this can be explained by the fact that the amplitude of the memristor voltage is maximum at this point, as shown in fig. 9(b). The voltage time series of fig. 9(b) show that the voltage amplitude increases up to the case where $\omega = \omega_0$, and after this point it decreases as voltage frequency is increased.

5 Conclusions

It is known that the model proposed by Strukov *et al.* [1] was introduced to qualitatively demonstrate the memristive behaviors. In this paper, we did a meticulous analysis of the numerical simulations using two different numerical methods (Adams-Bashforth and Runge-Kutta-Merson). We compared the numerical simulations with analytical solutions and SPICE simulations.

The results of sect. 4 raise a concern about the results obtained from numerical simulations. While the Runge-Kutta-Merson method provided solutions that changes with time. The Adams-Bashforth solutions usually evolved to a stationary state. When we compared the solutions with circuit emulators and analytical results, the Adams-Bashforth described the circuit emulators solutions with more precision and the Runge-Kutta-Merson described the analytical solutions better.

All methods evolved to similar solutions for the linear drift case, on the other hand, for the non-linear drift case, when the state variable spends time close to the borders of the domain, each method can evolve to a different state. Based on all the analyses we concluded that numerical simulations of memristor should be considered with caution.

The memristor coupled in series with an inductor and a capacitor preserves its pinched hysteresis loop. When the voltage frequency is increased, $\omega \gg 1$, the memristor behaves as a resistor. For low voltage frequencies values, $\omega < \omega_0$, we observe disagreement between the solutions of the methods considered in this work.

We thanks Araucaria Foundation, Capes (Finance code 001), CNPq, FAPESP (2015/07311-7) and UFVJM-PROACE for partial financial support.

Publisher's Note The EPJ Publishers remain neutral with regard to jurisdictional claims in published maps and institutional affiliations.

Appendix A. numerical methods to solve differential equations

In this paper, to solve differential equations were used two methods, one based on the Runge-Kutta's method and other based on Adam's method. Runge-Kutta's based methods are widely used because they require no specific set of initial conditions, demands low storage of data and the computational procedure is always the same [28]. Runge-Kutta's method are one-step methods, this means the former step depends only on the previous step, they are often called self-started. In contrast, Adam's based methods are multi-step, they require information about more than one previous state. The additional information on multi-step methods are expected to increase accuracy and stability [28].

In this appendix, we will present methods to solve the initial value problem:

$$\frac{dy}{dx} = f(x, y), \quad (\text{A.1})$$

$$y(x_0) = y_0. \quad (\text{A.2})$$

Runge-Kutta-Merson method

The Runge-Kutta-Merson method depends on 5 coefficients:

$$k_1 = hf(x_n, y_n), \quad (\text{A.3})$$

$$k_2 = hf(x_n + h/3, y_n + k_1/3), \quad (\text{A.4})$$

$$k_3 = hf(x_n + h/3, y_n + (k_1 + k_2)/6), \quad (\text{A.5})$$

$$k_4 = hf(x_n + h/2, y_n + (k_1 + 3k_3)/8), \quad (\text{A.6})$$

$$k_5 = hf\left(x_n + h, y_n + \frac{1}{2}(k_1 - 3k_3 + 4k_4)\right). \quad (\text{A.7})$$

In this case the solution for an equation like eq. (A.1) is given by

$$y_{n+1} = y_n + \frac{1}{6}(k_1 + 4k_4 + k_5). \quad (\text{A.8})$$

An advantage of this procedure is that if the differential equation (eq. (A.1)) is linear with x and y variables, then the error ε can be estimated as [29]

$$\varepsilon \sim \frac{1}{30}(2k_1 - 9k_3 + 8k_4 - k_5). \quad (\text{A.9})$$

Adams-Bashforth method

An alternative to the Runge-Kutta's based methods are the Adam's based methods that are multi-step. For Adams-Bashforth method the numerical solution for eq. (A.1) will be [28]:

$$y_{n+1} = y_n + \frac{h}{24}(55f(x_n, y_n) - 59f(x_{n-1}, y_{n-1}) + 37f(x_{n-2}, y_{n-2}) - 9f(x_{n-3}, y_{n-3})), \quad (\text{A.10})$$

h is the integration step, the local error is of order $\sim h^5$ and global error of order $\sim h^4$.

Appendix B. SPICE simulation

In this work, to emulate electric circuits, was used LTSpice. LTSpice is a freeware software from Linear Technology Corporation, now part of Analog Devices. The circuit was emulated using the SPICE code proposed by Biolek *et al.* [16].

References

1. D.B. Strukov, G.S. Snider, D.R. Stewart, R.S. Williams, *Nature* **453**, 80 (2008).
2. L.O. Chua, *IEEE T. Circ. Theor.* **18**, 507 (1971).
3. R.S. Williams, *IEEE Spectrum* **45**, 28 (2008).
4. J. Lee, B. Chen, S. Huang, M.J. Kushner, M.A. Zidan, Y.J. Jeong, W.D. Lu, *Nat. Electron.* **1**, 411 (2018).
5. P. Rabbani, R. Dehghani, N. Shahpari, *Microelectr. J.* **46**, 1283 (2015).
6. S. Sahoo, S.R.S. Prabaharan, *J. Nanosci. Nanotechnol.* **17**, 72 (2017).
7. S.P. Adhikari, M.P. Sah, H. Kim, L.O. Chua, *IEEE Trans. Circ. I* **60**, 3008 (2013).
8. J. Luo, X. Xu, Y. Ding, Y. Yuan, B. Yang, K. Sun, L. Yin, *Eur. Phys. J. Plus* **133**, 239 (2018).
9. C.P. Uzunoglu, Y. Babacan, F. Kacar, M. Ugur, *Electr. Power Compon. Syst.* **44**, 638 (2016).
10. M. Potrebic, D. Tosic, *Radioengineering* **24**, 408 (2015).
11. I. Sinclair, *Passive Components for Circuit Design*, 1st ed. (Newnes, Oxford, 2001).
12. K.M. Sundqvist, D.K. Ferry, L.B. Kish, *Fluct. Noise Lett.* **16**, 1771001 (2017).
13. K.M. Sundqvist, D.K. Ferry, L.B. Kish, *Phys. Lett. A* **381**, 3364 (2017).
14. I. Abraham, *Sci. Rep.* **8**, 10972 (2018).
15. I.D. Mayergoyz, W. Lawson, *Basic Electric Circuit Theory*, 1st ed. (Academic Press, Cambridge, MA, 1997).
16. Z. Biolek, D. Biolek, V. Biolková, *Radioengineering* **18**, 210 (2009).
17. Y.N. Joglekar, S.J. Wolf, *Eur. J. Phys.* **30**, 661 (2009).
18. M.D. Pickett, D.B. Strukov, J.L. Borghetti, J.J. Yang, G.S. Snider, D.R. Stewart, R.S. Williams, *J. Appl. Phys.* **106**, 074508 (2009).
19. C. Yakopcic, T.M. Taha, G. Subramanyam, R.E. Pino, S. Rogers, *IEEE Electron. Dev. L.* **32**, 1436 (2011).
20. T. Prodromakis, B.P. Peh, C. Papavassiliou, C. Toumazou, *IEEE Trans. Electron. Dev.* **58**, 3099 (2011).
21. H. Kim, M.Pd. Sah, C. Yang, S. Cho, L.O. Chua, *IEEE Trans. Circ.-I* **59**, 2422 (2012).
22. S. Kvatinsky, E.G. Friedman, A. Kolodny, U.C. Weiser, *IEEE Trans. Circ. Syst.* **60**, 211 (2013).
23. V.S. Baghel, S. Akashe, *J. Active Pass. Dev.* **11**, 89 (2016).
24. A. Ascoli, R. Tetzlaff, Z. Biolek, Z. Kolka, V. Biolková, B. Biolek, *IEEE J. Em. Sel. Top. C* **5**, 133 (2015).
25. L. Chua, *Proc. IEEE* **100**, 1920 (2012).
26. L. Chua, *Appl. Phys. A* **102**, 765 (2011).
27. J.W. Nilsson, S.A. Riedel, *Electric Circuits*, 8th ed. (Pearson Prentice Hall, 2008).
28. E. Kreyszig, *Advanced Engeneering Mathematics*, 9th ed. (John Wiley & Sons, Singapore, 2010).
29. R.E. Scraton, *Comput. J.* **7**, 246 (1964).